Hybrid Solar-RF Energy Harvesting Mechanisms for Remote Sensing Devices

Hoang T. Tran*, Minh T. Nguyen**‡, Cuong V. Nguyen***, Guido Ala****, Fabio Viola****, Ilhami Colak*****

* Center of Electrical Engineering, Duy Tan University, Danang, 550000, Vietnam.

** Department of Electrical Engineering, Thai Nguyen University of Technology, Thai Nguyen 240000, Vietnam.

*** Department of Electronics and Communications Technology, Thai Nguyen University of Information and Communication Technology, Thai Nguyen 240000, Vietnam.

**** Department of Engineering, University of Palermo, Viale delle Scienze, Parco d'Orleans, 90128 Palermo PA, Italy.

***** Department of Electrical and Electronics Engineering, Nisantasi University, 34398 Instanbul, Turkey.

(tranthuanhoang@duytan.edu.vn, nguyentuanminh@tnut.edu.vn, nvcuong@ictu.edu.vn, guido.ala@unipa.it, fabio.viola@unipa.it, ilhcol@gmail.com)

‡ Corresponding Author: nguyentuanminh@tnut.edu.vn, Thai Nguyen 240000, Vietnam, Tel: +84 2083847093.

Received: 11.02.2021 Accepted: 07.03.2022

Abstract- Recently, sensor networks effectively provide many applications in different fields. The deployment of mobile sensors, unmanned aerial vehicles is to reduce the burden of energy consumption for sensor nodes. However, saving energy in such networks is still a critical issue. This paper investigates the performance of a hybrid RF-Solar harvesting circuit for remote sensing devices. The harvesting circuit can simultaneously harvest power from solar and radio frequency (RF) sources readily available in the surrounding environment. The proposed work builds RF and solar harvester circuits to create hybrid harvesting circuits for all elements in the combined sensing networks. The stand-alone RF harvester circuit is a dual-band multi-stage harvester that is designed to work at 2.4GHz, Wi-Fi/WLAN bands. The standalone solar harvester circuit comprises a solar panel with a maximum power point tracking (MPPT) algorithm. The whole hybrid system can produce a maximum power of up to 133.25W with a boost current element in the charging system. Since each node is equipped with a rechargeable battery, all the batteries are charged by the harvested power from the proposed circuits. This approach supports the operation of the networks safe and continuous even when a shortage of harvested power happens due to bad conditions such as cloudy or rainy days. This work shows promise and is applicable.

Keywords- Hybrid energy harvesting, Wireless sensor networks, Solar energy, RF energy, Mobile sinks, Unmanned aerial vehicles.

1. Introduction

Wireless sensor networks (WSNs) are infiltrating the environment in its wide sense, indoors and outdoors, in the human body, in unapproachable emplacements; they have found their way into a wide variety of applications and systems with vastly varying requirements and characteristics such as health, military, inter-vehicular, and infrastructure monitoring applications [1,4]. However, the problem of power consumption is always one of the pressing issues as these networks operate almost by using pre-charged batteries. Sensing devices will stop working and cause loss of connectivity between networks if they run out of energy storage. This has prompted many research projects on the problem. Especially, energy-saving routing methods to prolong the network lifetime [5,8].

In the literature, the researchers focusing on data collection methods have been well conducted. Numerous methods such as random walk, tree-based routing, shortest paths, etc have been studied in [9,11]. These methods aim to diminish communication costs by reducing the number of hops routing. Excessive sensing data also cause notable energy waste. Minimizing sensing data sent by sensor nodes are widely studied to deal with excessive data problems [12]. In [13], an AI-based data processing algorithm is proposed. This algorithm separates sensing data into two categories static and dynamic data. Static data are transmitted to sever-sides, after that only moving dynamic data are updated to reduce data transmission cost. Mobile sensors are deployed to support the static sensors with either the mobile flexible features or capable of handling longer communication distances [14,16]. This deployment saves significant energy for static nodes. Unmanned aerial vehicles (UAVs) are often used in WSNs in some specific cases as mobile base-station

(BS) to support directly either static sensor nodes or mobile robots handling long- distance communications [17,18].

Scheduling mechanisms are also investigated to enhance power-efficient of sensor networks. The idea of this method is that some sensor nodes are chosen to be active and have full functions while the rest of the sensor nodes can be in sleep mode to save energy [19,20]. All of the aforementioned methods prove the effectiveness in reducing total energy expenditure for sensor networks. However, implementing advanced algorithms normally requires complicated computation. This feature is undesired in practices where sensor nodes are small and have limited computational ability. In addition, these methods still depend on pre-charged batteries and do not consider the recharging approach. In this situation, the energy harvesting (EH) approach emerges as a potential candidate to tackle energy problems for WSNs. This method does not require performing complex algorithms. In addition, EH can provide a convenient power supply for wireless devices by exploiting ambient energy sources such as solar, vibrant, wind, RF energy, and harvesting rainfall energy [21,24]. In [25], the authors give requirements on the energy of sensor nodes, and then the authors propose a method to harvest energy from electric and magnetic fields from surrounding electrical equipment. By applying the proposed method, the obtained capacity of power sources is about 250mW, which is also a promising solution to supply power to sensor nodes in the network. In [26, 27], the authors propose a method to harvest wind energy to provide sensor devices that monitor temperature and vibration in bogies in the wireless sensor networks. The authors utilize the energy obtained while the train and vehicles are running at a speed from 35km/h to 90km/h, the voltage obtained is from 3.3V- 22V. In [28], a hybrid energy scheme is proposed. Solar energy is combined with RF energy only at 2.4GHz to overcome the limitations of RF energy and create a charger with a maximum charging capacity of 9W. In [29], the authors propose to reduce the size and energy consumption of electronic devices in the sensor network, and at the same time, the authors also propose a method to harvest energy from solar, thermal, mechanical energy sources to power these electronics. A method harvesting solar and RF energy at 900MHz and 2.4GHz for powering Base Transceiver Stations (BTS) is proposed in [30, 31]. In [32], the authors propose a method to harvest energy from solar energy and design the charging system for the battery that the sensor nodes use, but the authors do not mention in detail the parameters of the solar panel, and the battery. So, it is difficult to evaluate the efficiency of the energy collection process.

In addition, in recent years, many researchers have focused on improving the conversion efficiency from RF-DC power sources. In [33], the authors focused on improving the conversion efficiency from RF energy to DC power and achieved 52.1% efficiency while in paper [34] only achieved 40% efficiency. In [35] the authors proposed a method to collect RF energy at 900MHz and achieve conversion efficiency from RF-DC energy of 73%.

The previous studies mostly give general solutions for wireless sensor networks. They do not give details on the components in the sensor network built on how much energy is consumed. Besides, they also have not yet combined two sources of RF-solar energy together to ensure the stability of the power supply. In this work, based on the results of these studies, we propose a solution to power sensing devices in wireless sensor networks from ambient energy sources. Energy harvesting techniques, energy sources, storage technology, charging technology are presented in detail. The proposed method is implemented to reduce the charging time of batteries for static devices (Sensor Nodes) and mobile devices (Relay Nodes and Sink nodes). A similar system has as its motivation to guarantee the continuity of operation in systems for which access to a continuous source of energy is precluded. This situation can be found in areas where for ecological reasons or landscape constraints and to preserve the integrity of the artistic structures the use of energy on conductors is to be excluded.

In short, our contributions are addressed as follows.

a) A hybrid method that can harvest both RF and Solar energies is proposed to clear out disadvantages of each separated system and to supply sensing devices more stably.

b) MPPT algorithms are built and simulated that support solar panels always working at the Maximum Power Points.

c) A new charging system is designed to keep the voltage stable from 18V-24V and to increase the charging current up to 6.5A that helps the charging process faster.

The rest of the paper is organized as follows. Section 2 describes the system model. Section 3 addresses the proposed method, the concepts, and the elements in the system presented in detail. All simulation results of the hybrid system including charging current and charging voltage for each type of device are provided in Section 4. Finally, the conclusions and future developments of the paper are addressed in Section 5.

2. System Model

As mentioned, the energy consumption problem in WSNs is always critical. Hence, the issue of replenishing and powering energy in such networks is so crucial that it motivates our work to propose a combined energy harvesting system for further applications. Figure 1 shows an overview of the system model including static sensor nodes and mobile devices. In this work, both solar and RF energy are collected and then converted into electricity to partly power the remote sensing system. In the case of using only solar energy, the weakness of this energy source is that it depends a lot on weather conditions as mentioned in [36].

The proposed hybrid harvesting model including RF energy overcomes this situation in which the RF energy is converted from the AC signal energy to DC power that simultaneously supports the devices. The output of these two EH receivers will be hybridized to the charging system. The task of the charging system is to stabilize the output voltage and current while boosting the charging current. The stabilizer supports the charging voltage and charging current being stable to power the sensor nodes, mobile robots, and the unmanned aerial vehicles in the sensing system. In addition, the system is designed for long-term data collection applications in areas that are difficult to be reached by humans. Hence, the system needs to be designed suitable to all the devices working in the field.

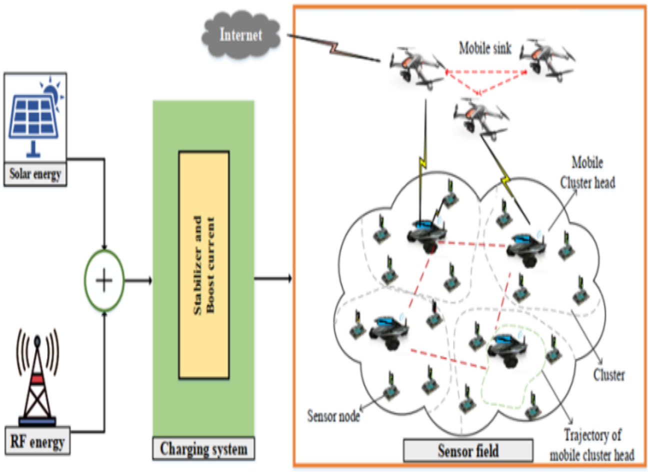

Fig. 1. The combined model includes the hybrid energy harvesting system for all sensor nodes, mobile robots (mobile cluster heads) and unmanned aerial vehicles - UAVs (or mobile sinks).

In this model, we apply the case of equal clustering. For example, the K-mean algorithm is mentioned in [37]. The use of equal clustering will have some benefit in this case because we use the mobile sink and the mobile cluster head to collect data from the sensor nodes. Because of the inductance, there is no feature that the cluster heads near the sink have to move with large amounts of data so we do not consider the balance of energy. If applying an uneven clustering algorithm, in this case, wasted the computational resources and the introduction of mobile sinks and mobile cluster heads has no meaning. The mobile cluster heads will be controlled to follow a path as [38] to collect data. At this point, the sensor nodes (SN) must have a scheduling algorithm so that when the mobile cluster head (MCH) moves to the communication distance, these nodes receive the beacon and turn on the active mode, before a transmission. After the data transmitting steps between SN and MCH are finished, SN may go to sleep immediately to save energy consumption. This issue will be addressed in another work out of this paper. The mobile sink (MS) or UAVs work similarly to the MCH, which collects data from MCHs. The design and configuration of the elements in the sensor network are described in Section 3 of this paper.

3. The Proposed Methods

As shown in the system model, the devices have different levels of energy consumption. Based on different functions and energy consumption of electronic devices in the networks, we propose a different power supply for each device. The detailed design for each type is addressed as follows.

3.1. Solar Energy Harvesting

The solar cell's output voltage requires a booster converter to upgrade the voltage according to your needs and purpose. There are many turbocharged converters out there, but the most common and simplest is the Boost converter. In addition, to ensure the full use of the capacity of the solar cell, it is necessary to use the MPPT algorithm in the Boost converter control system. In this section, we will build the Boost converter system and the MPPT algorithm used in the solar energy system.

3.1.1. The Principle of The Boost Converter

A booster converter is a universal DC/DC converter that is typically applicable for applications where the output voltage is higher than the input voltage. The popular supercharger is the Boost converter. For simplicity in the analysis of the operating principle of the Boost transformer, we consider the ideal Boost converter (ignoring the effect of resistance RL in the inductor, RESR in the capacitor) as shown in Figure 2a.

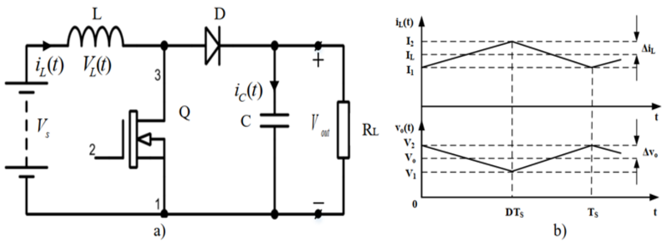

Fig. 2. The boost converter

The current form $i_L(t)$ and output voltage $v_{out}(t)$ are shown in Figure 2b as follows.

During T_{on}: Q_1 opens and D locks, the current direction $i_L(t)$ through the inductor and $i_c(t)$ through the capacitor as shown in Figure 3a as follows.

The supply voltage is represented as

$$V_s = \frac{L(I_2 - I_1)}{T_{on}} = \frac{2L\Delta I_L}{T_{on}}. \quad (1)$$

From Equation (1), we have

$$\Delta I_L = \frac{V_s\, T_{on}}{2L}. \quad (2)$$

The current going through the capacitor can be calculated as

$$i_c = C\frac{V_1 - V_2}{T_{on}} = C\frac{-2\Delta V_{out}}{T_{on}} = \frac{-V_{out}}{R_t}, \quad (3)$$

where $$C = \frac{V_{out}T_{on}}{2R_t\Delta V_{out}}. \quad (4)$$

During T_{off}: Q_1 locks and D opens as shown in Figure 3b above.

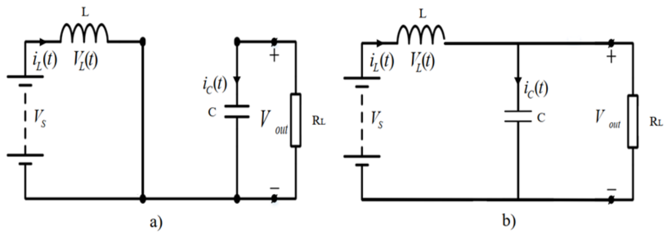

Fig. 3. Equivalent circuit when the state Q1 and diode D change

We have the formula for the balanced voltage as

$$V_s - V_{out} = L\frac{I_1 - I_2}{T_{off}} \ or\ V_s - V_{out} = L\frac{2\Delta I_L}{T_{off}}. \quad (5)$$

The current going through the capacitor can be calculated as

$$i_C = C\frac{2\Delta V_{out}}{T_{off}} = I_L - \frac{V_{out}}{R_t}. \quad (6)$$

From Equation (5), we have

$$\Delta I_L = \frac{(V_{out} - V_s)T_{off}}{2L}. \quad (7)$$

From Equation (2) and Equation (7), we can have

$$\frac{V_S T_{on}}{2L} = \frac{(V_{out} - V_s)T_{off}}{2L}, \quad (8)$$

where $$D = \frac{T_{on}}{T_{on} + T_{off}} \quad (9)$$

Replacing the D into Equation (8), we can achieve

$$V_{out} = \frac{V_s}{1-D}. \quad (10)$$

Assuming that power loss is zero, we have

$$V_s I_L = V_{out} I_{out}.$$

(11) From Equation (10) and Equation (11), the I_L can be calculated as

$$I_L = \frac{I_{out}}{1-D}. \quad (12)$$

From Equation (2) and Equation (4), the L and C can be calculated as

$$L = \frac{V_s T_{on}}{2\Delta I_L} = \frac{V_s T_{on} D}{2D\Delta I_L} = \frac{V_s T D}{2\Delta I_L} = \frac{V_s D}{2 f_s \Delta I_L}, \quad (13)$$

$$C = \frac{V_{out} D T_{on}}{2R_t \Delta V_{out}} = \frac{V_{out} D T}{2R_t \Delta V_{out}} = \frac{V_{out} D}{2 f_s R_t \Delta V_{out}}, \quad (14)$$

where f_s is the switching frequency (switching) of the switching valve.

3.1.2. The MPPT algorithm

There are many MPPT (Maximum Power Point Tracking) algorithms that are found out, of which there are two popular algorithms: Perturb and observe algorithm (P&O algorithm) and Incremental conductance algorithm (INC algorithm). In this paper, we use the P&O algorithm to control the D modulation coefficient directly.

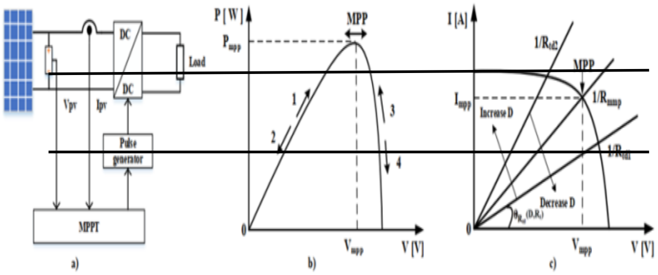

Fig. 4. Solar cells with P&O algorithm directly control the D modulation coefficient.

. The working point of a solar panel is the intersection between the I-V characteristic line of the solar panel and the I-V characteristic line of the load. We consider the load as pure impedance so that the characteristic line is a straight line with a slope of 1/R. Assuming there are three values of the load, R1, R2, R3, the three I-V characteristic lines will have slopes of 1/R1, 1/R2, 1/R3 respectively. In which only the I-V characteristic lines of R2 load intersects the I-V characteristic line of the solar panel at MPP as shown in Figure 4c.

There is only one MPP for each certain weather condition. Moreover, when the weather conditions change, the MPP also changes. Thus, to optimize the performance of the solar panel, it is necessary to keep the solar panel working at the MPP. The Maximum Power Point Tracker controller will perform that task by controlling the opening and closing of the DC/DC converter valve as shown in Figure 4a.

Changing the position of the working point by changing the angle of inclination $\theta_{Rtd}(D, R_t)$ means changing the modulation factor D. A reasonable change in D will obtain the intersection of two characteristic lines established at the correct MPP, where

$$\theta_{Rtd}(D, R_t) = \text{atan}\left(\frac{1}{(1-D)^2 R_t}\right). \quad (15)$$

From Figure 4b and Figure 4c we have

- ➢ If the operating point of the system is moving in direction 1 in Figure 4b, it means ΔP > 0 and ΔV > 0 the corresponding point of operation is to the left of the MPP point. Then the angle of inclination θ_Rtd (D,R_t) in Figure 4c will decrease so that the operating point moves towards the MPP point resulting in a decrease in the modulation factor D.
- ➢ If the operating point of the system is moving in direction 2, it means ΔP< 0 and ΔV< 0 and, the operating point is to the left of the MPP point. Then the angle of inclination θ_Rtd (D,R_t) will decrease leading to a decrease I n the modulation factor D.
- ➢ If the operating point of the system is moving in direction 3, it means ΔP > 0 and ΔV < 0, the operating point is to the right of MPP. Similarly, the modulation coefficient D increases.
- ➢ If the operating point of the system is moving in direction 4, it means ΔP < 0 and ΔV > 0, the operating point is to the right of the MPP point. Then the modulation coefficient D increases.

From the above analysis we proposed an algorithm as follows:

Algorithm 1: Modulation coefficient adjustment algorithm (P&O)

Output: Value of current and power

Phase 1. Measure current and voltage values output at time K of the solar panel

Phase 2. Calculate P(k) =V(k) * I(k), ΔP = P(k) **-** P(k-1), ΔV= V(k)-V(k-1)

Phase 3.

If ΔP > 0 and ΔV > 0 or ΔP < 0 and ΔV < 0 → reduces duty cycle of D

If ΔP > 0 and ΔV < 0 or ΔP < 0 and ΔV > 0 → increases duty cycle of D

Phase 4. Update the current and power values and perform the next cycles.

The process of building a simulation of the MPPT algorithm is shown in Figure 5.

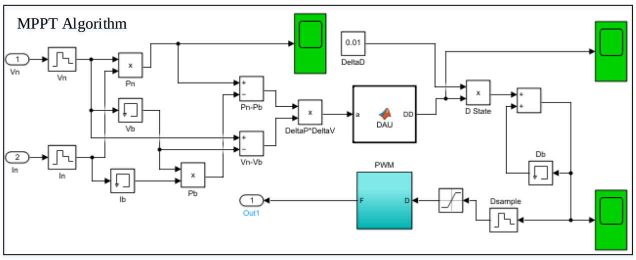

Fig.5. Building MPPT algorithm on Simulink

3.2. RF Energy Harvesting

The whole concept of the RF energy collection system is shown in Figure 6 including Harvesting RF energy for sensor node Figure 6a), Harvesting RF energy for relay nodes or mobile sensors Figure 6b), and Harvesting RF energy for sink node or UAVs Figure 6c). The main elements are antennas, matching circuits, and rectifiers which are addressed in detail as follows.

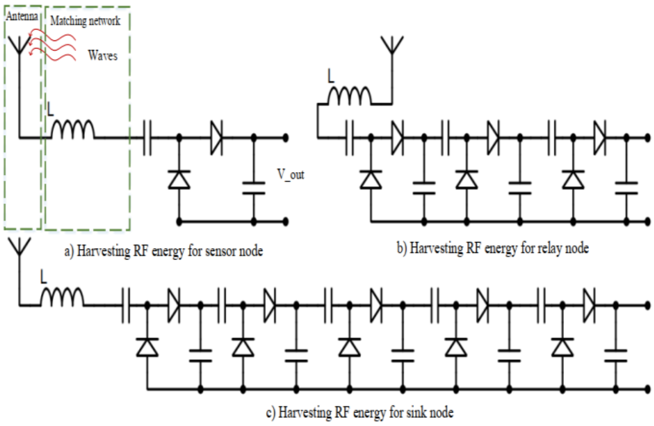

Fig. 6. RF energy harvesting circuits

Antennas are often designed for transmitting and receiving different kinds of signals. In this work, they are also the devices in the radio frequency (RF) energy harvesting (EH) circuits that capture RF signals to be converted to energy. The effectiveness of antennas is a key factor relating to operating frequencies and supporting to guarantee the high performance of EH systems. The RF antennas can harvest energy from different resources, such as cellphones (GSM 850/900/1800/1900/UMTS), local area networks (2.4–5.9 GHz), Wi-Fi signals, and broadcast ultra-high-frequencies (UHF) of TV signals. The amount of each EH system depends on either the sizes, the arrangement of antennas, selected frequencies, or other related elements as matching circuits.

Normally, matching circuits are designed for the best possible impedance match. Hence, the main function of this circuit is to maximize the input voltage of the rectifier and to diminish the transmission loss from antennas to rectifiers.

When the impedance of loads and impedance at antenna output is matched, the maximum power transfer could be obtained. The matching circuits in this work are designed to reach the goal. In our work, a matching circuit is designed for RF waves with a frequency of 2.4GHz.

Table 1. Matching network parameters.

Order	Parameter	Value	Unit
1	Z_0	50	Ω
2	Z_S	50	Ω
3	Z_L	50+60j	Ω
4	L	3.98	nH
5	f	2.4	GHz

Assuming the circuit has the following parameters as in Table 1, where Z_S the is impedance of the source, Z_0 is the impedance of the transmission line, and Z_L is the impedance of a load. A load is composed of a resistor R= 50 Ω connecting in series with a capacitor C= 1,106pF. The load impedance is Z_L= 50-60j (Ω). Inductance (L) for the matching circuit has been determined by the Smith chart. Then, the design of the matching circuit was verified by simulations using ADS (Advanced Design System) software. The matching circuit has been designed as in Figure 7.

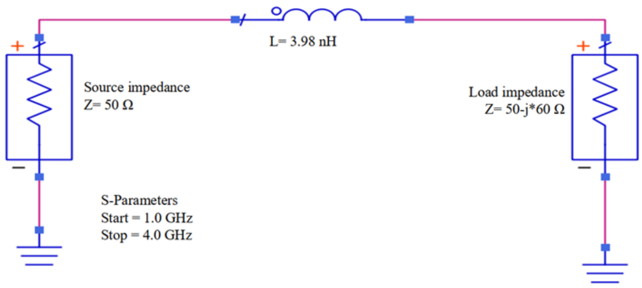

Fig. 7. Matching network.

The return loss dB(S(11)) presents a measure of power signal loss because of signal reflection by a discontinuity in a transmission line or optical fiber. Insertion loss dB(S(21)) is a power signal loss resulting from inserting an external device into a transmission line or optical fiber. Both return loss and insertion loss are measured in decibel dB. The simulation results are given in Figure 8. At the desired frequency of 2.4GHz, Insertion loss is approximately 0dB, while Return loss goes to -75dB. The results imply that nearly 100% of the signal from input goes to output without loss. By the smith chart, the impedance is obtained as Z_0*(1+0j), which fulfills our expectations. As the input is matched with the characteristic impedance Z_0, the reflection coefficient goes to 0.

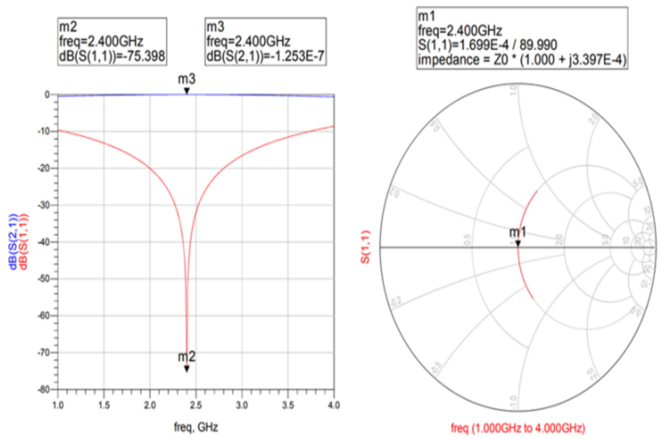

Fig. 8. The impedance Smith Chart.

At the last stage, rectifier circuits are used to obtain DC voltage from harvested RF energy [39]. The challenge in implementing a rectifier circuit is that the circuit must provide a suitable and reliable output voltage under the variation of RF energy sources in the environment. In rectifiers, circuits and diodes are critical factors that affect the conversion performance. Thus, diodes should be carefully selected when designing a rectifier circuit. In general, diodes with low voltage are desired for high-efficiency rectifier circuits.

The number of rectifier stages has a great influence on the output voltage of the energy harvesting circuit. In this paper, we design the system in three types of architecture to suit each type of node. Type one stage that uses the sensor node as shown in Figure 6a, type three stages used for the relay node as shown in Figure 6b, and type 5 stages used for sink nodes as shown in Figure 6c. The output voltage and power of each of these architectures are different to suit the power consumption of the nodes mentioned in the next section.

3.3. Charging system

In Figure 9, we design a charging system with the following components: *SUM, TIP147, LM317T*, $C_1 = 1000\mu F$, $R_1 = 10\Omega$; $R_2 = 150\Omega$; $R_3 = 8\Omega$. The charging system includes a boost current and stabilizer. Solar-RF energy sources, after being put into the Hybrid, the current will be boosted through the boost converter, with the effect of reducing the charging time of the battery. However, to ensure that the charging current and charging voltage is always stable, they are put through a stabilizer. We know that the charging process of the battery is divided into two phases: firstly, the battery is charged with constant current, when it reaches about 80 %, the battery switches to charging mode by voltage. Therefore, we need to balance these two factors to ensure the fastest charging process possible. The principle of operation is shown in Figure 9. The main function of this system is to ensure the voltage is kept stable from 18-24V and increase the charging current for the battery up to 6.5 A.

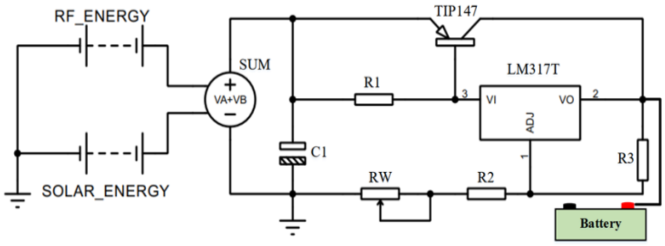

Fig. 9. Hybrid charging system with output stabilizer.

3.4. Sensor Field

In wireless sensor networks, there are many types of nodes that the power consumption varies. Most of these nodes are divided into 3 types, including sensor node, relay node, sink node. In general, they have consumption capacity as shown in Table 2. For each node type, some batteries are suitable for each node to power them, in this article we propose three types of batteries corresponding to the three types of nodes as shown in Table 2.

4. Results and Discussion

In this section, the paper simulates the stand-alone solar and RF energy harvesting, we show some issues of the stand-alone energy harvesting system. To tackle these issues, the power supplying system is carried out as hybrid solar-RF energy. With the purpose to meet the energy demand for devices in the wireless sensor network, all the output values of the energy hybrid must be adjusted by the charging system.

4.1. Solar Stand-Alone

Solar energy is the main power supply for the devices in wireless sensor networks. We utilize the KS5M-36 solar panel of Kingstar brand which has the basic parameters at standard conditions (1000W/m2 at 25°C) as the following Table3. A simulation model of the solar harvesting system and Boost converter using the MPPT algorithm is shown in Figure 10. The MPPT algorithm requires output voltage and current after solar panel system to calculate the instantaneous power to give a suitable value of D, the MPPT algorithm simulated on Matlab/Simulink.

The simulation results, in this case, are shown in Figure 11. I-V characteristics and P-V characteristics show that solar panels work at Maximum Power Point. The P&O algorithm is used to make the solar panel always work at the maximum power point. However, the output voltage value of the Boost converter will change with the light intensity, this leads to the need for another converter to stabilize the output voltage of the Boost converter to provide a stable source from 18-24V for the device's power system. As analyzed in the previous section, the boost current and stabilizer are chosen to keep the voltage stable and increase the charging current for the battery. The output voltage of the solar panel system using the MPPT algorithm will be put to the input of the hybrid system as shown in Figure 9.

Table 2. Specifications of the nodes

Parameter		Type	Manufacturer	Power (mW), Current (mA) consumption or Capacity (Ah)	
				Active or TX	Sleep or RX
Sensor node	MCU	ATxmage	ATmel	1.1 mA	0.7 µA
	Gas sensor	DTK-2	NTC-Russia	120 mW	
	Transceiver	CC2500	Texas Instrument	21.1 mA	13.3 mA
	Battery	SLA	Gens Ace	1.3 Ah	
Mobile cluster head	Mobile robot	Rovio	WowWee		
	MCU	ATmega	ATmel	1.8 mA	0.9 µA
	Transceiver	CC2430	Texas Instrument	27 mA	25 mA
	Battery	3S Li-Po	Gens Ace	3 Ah	
Mobile sink node	UAV	M200 V2	DJI	13 W	
	Transceiver	CC2430	Texas Instrument	27 mA	25 mA
	Ethernet	ESP 8266		215 mA	60 mA
	Battery	6S Li-Po	Gens Ace	7.66 Ah	

The results show that solar energy harvesting systems are significantly affected by environmental conditions. Therefore, other sources of energy are required to assist in the face of adverse environmental conditions. In this paper, we use the RF energy combined with it to remedy this situation.

Table 3. Parameters of the solar cell Ks5M-36 measured in standard conditions (solar radiation intensity 1000W/m2, temperature 25ºC).

Parameters	Symbol	Value
Power	P_{MPP}	5 W
Voltage at Maximum Power (VMPP)	V_{MPP}	17.6 V
Current at Maximum Power (IMPP)	I_{MPP}	0.28 A
Open Circuit Voltage (VOC)	V_{OC}	22 V
Short Circuit Current (ISC)	I_{SC}	0.31 A

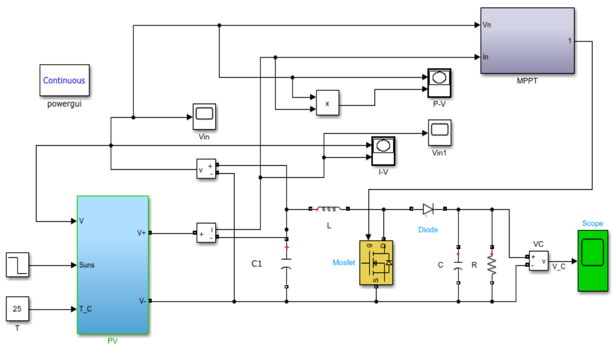

Fig. 10. The scheme of the stand-alone harvesting solar energy with MPPT algorithm.

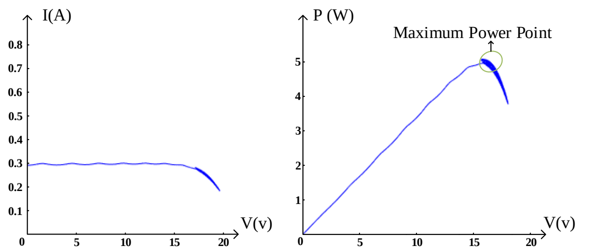

Fig.11. The output of solar harvesting system using MPPT algorithm

4.2. RF Stand-Alone

In Figure 12 the black lines correspond to the output voltages of the RF energy collection circuit with one stage. The blue line corresponds to the output voltage of the RF energy gathering circuit with the three stages. The red line corresponds to the output voltage of the RF energy-gathering circuit with five stages. After about 35 seconds, the output voltage reaches a stable value of 1.48V, 3.23V, 5.06V, respectively. These voltages are too small to supply the battery and the output current with the five-stage circuit is also too small. So if only one RF power source is used, it will not be enough to charge the battery. But the RF energy source has the advantage of less dependence on the surrounding environment than the solar source. Therefore, we propose a hybrid solar and RF energy system.

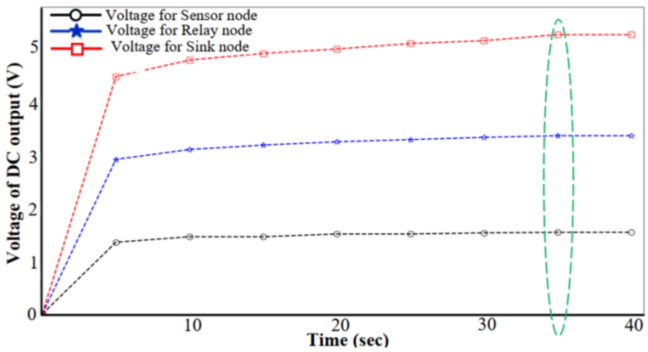

Fig. 12. Output voltage of RF energy harvesting circuit.

4.3. Hybrid Solar-RF Energy Harvesting

In Figure 13 a) and Figure 13 b) are the voltage and current supplied to the sensor node, the output voltage of the single-stage RF energy collector circuit hybrid with solar energy through the boost converter and stabilizer, we get the charging current is 1.26A and the charging voltage is 6.30V for Sensor Nodes. Besides, Figure 13 c) shows the battery charging process that supplies power to sensor nodes. This process is divided into 2 phases. In the first phase, the battery is charged by a constant current charge (CC Charge). When the battery is 80% charged and wants to reach 100% the battery should switch to the charging state with constant voltage charge (CV Charge). In the first phase, the battery charge to t =1600s.

Time from the 1600s to 2000s is the second stage of the battery charging and the battery is fully charged at about 2000s with the charging current of 1.26A and the charging voltage of 6.30V in the case of Sensor Nodes. However, in this paper, we have assumed that when the state of charge (SoC) of a battery gets down to 50% it starts to be recharged. So, the above time is the charging time from SoC is from 50% to 100% While the battery is charging, the battery voltage will increase.

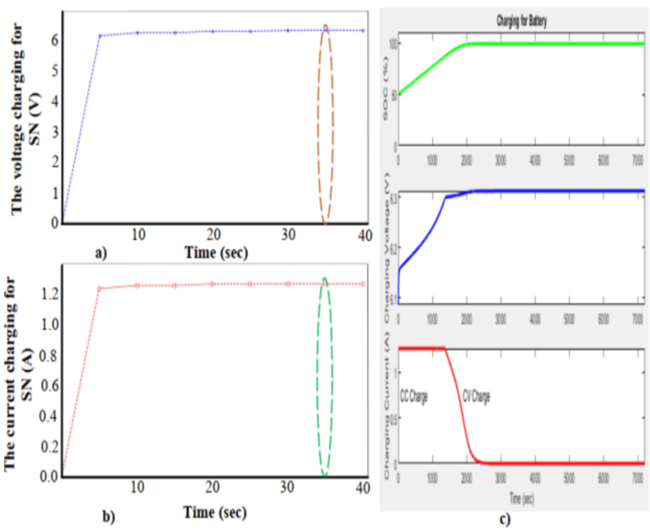

Fig.13. Charging for Sensor nodes.

The charging process of mobile cluster heads is depicted in Figure 14. The charging current and charging voltage for Mobile Cluster Head is 2.37A and 11.9V respectively. Under the same assumption, the cluster heads start charging as the SoC of the battery falls below 50%.

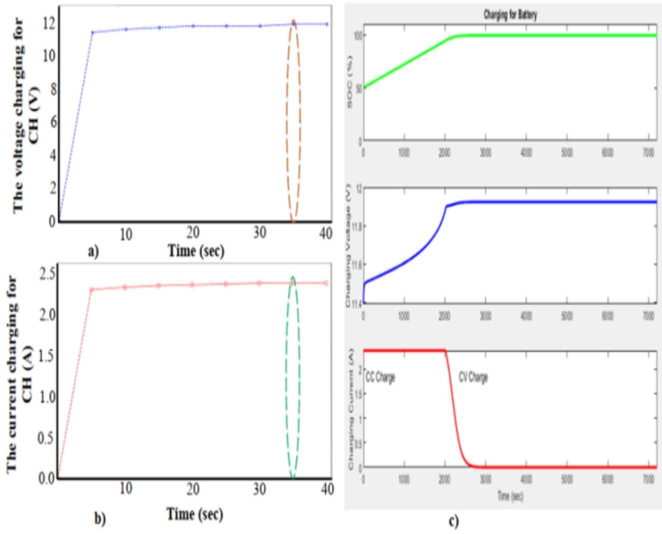

Fig.14. Charging for Relay nodes.

The battery is rapidly charged to 80% by the current in approximately the 2000s. Then, the second stage gradually charges the remaining capacity using the charging voltage. The second stage takes nearly 300s to complete.

An identical charging mechanism is applied to charge the battery for the sink. From Figure 15 a) and figure 15 b), the charging current and charging voltage for Mobile Cluster Head are 6.5A and 20.5V respectively. The SoC rises to 80% from 50% in 1800s by the current charging in the first stage. The battery is fully charged at t = 2000s.

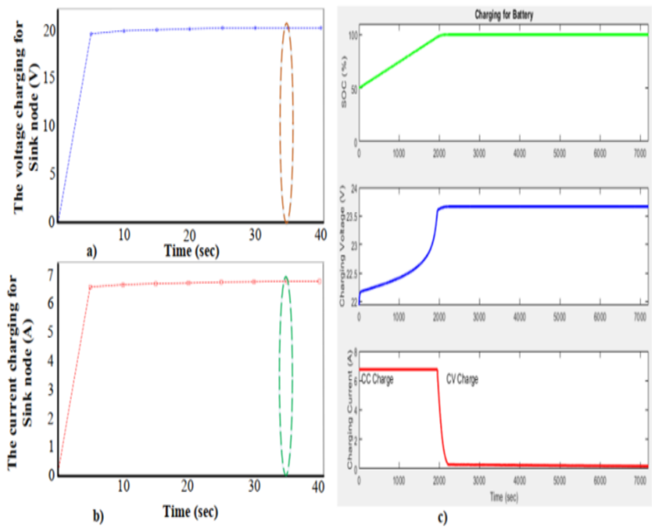

Fig. 15. Charging for the Sink nodes

In this application, we assume the load with 18V- 24V in any case. The battery is in discharge mode, SoC is decreasing and the battery current is positive. The system separately works for two cases. To do this we use a switch, which will determine the mode of charging or discharging. It should work based on voltage sources which are harvested from ambient energy as mentioned above. When the source is enabled, the battery is charging and load is supplied from this source. When the source disables, the battery is in discharge mode, the load is supplied from the battery.

Table 4. Comparison some existing results to our results

Method	V_{RF}	V_{Solar}	V_{Hybrid}
Hybrid Solar and Radio Frequency (RF) Energy Harvesting [28]	4.5V	8V	12V
Improved RF to DC energy conversion efficiency [40, 41]	0.3V- 2.2V	0.5V- 6.1V	0.7V-7.8V
Collect energy from single energy sources: solar energy and RF energy efficiency [42, 43, 44]	3.2V- 5V	8V-21.6V	None
Our proposed method	5.06V	17.6 V	20.5 V

Table 4 compares our proposed approach with some recent studies. In [28] the authors present a hybrid harvesting approach for RF and solar energies, but specific applications are not investigated. In [40, 41] the authors mainly focus on improving the conversion efficiency from RF energy to DC. Therefore, the authors do not use as many stages as other studies. The author is only interested in increasing the output voltage by increasing the conversion efficiency from RF to DC. In [42, 44], the authors mainly focused on harvesting RF stand-alone or solar stand-alone sources without any interest in combining the two sources. Our results overcome the existing ones and show promise in the specific applications and hope for further developments in the near future.

5. Conclusion and Future Developments

In this paper, we have proposed a system that effectively combines RF and solar energies. In fact, there are different scenarios that the sensing devices operate and need extra energy resources. Hence, we have designed the hybrid energy harvesting system to accommodate different types of batteries, corresponding to different devices in such networks. Therefore, our system can generate stable charging voltage and charging current 20.5V, 6.5A for the devices in wireless sensor networks. With that charging current and voltage, it makes the charging process faster and more efficient. The charging stages of the battery are also outlined in this paper. Some significant results are provided to verify the problems. The proposed approach shows the potential solution for increasing the lifetime of sensor networks by utilizing energy sources that are abundant in ambient environments.

To improve system performance, the conversion efficiency from solar energy and RF energy to DC power is also very important. The advanced MPPT algorithms based on heuristic algorithms such as fuzzy logic would be the next steps in future research. The switching loss due to the semiconductor switches in boots and stabilizer circuits will also be taken into account in designing control schemes for these switches. Besides, the control of multiple mobile agents in the network will be considered to avoid collisions and minimize their power as agents travel. In future work, we will study to find a mathematical model to represent the dependence of load power consumption with the power supply capacity, which varies in different conditions of the surrounding environments.

Acknowledgements

Authors would like to thank Thai Nguyen University of Technology (TNUT), Viet Nam for the support.

References

[1] M. T. Nguyen, C. V. Nguyen, H. T. Do, H. T. Hua, T. A. Tran, A. D. Nguyen, G. Ala, and F. Viola, “Uav-assisted data collection in wireless sensor networks: A comprehensive survey,” Electronics, vol. 10, no. 21, p. 2603, 2021.

[2] M. Khanafer, M. Guennoun, and H. T. Mouftah, “Wsn architectures for intelligent transportation systems,” in 2009 3rd International Conference on New Technologies, Mobility and Security, IEEE, pp. 1–8, 2009.

[3] M. A. Hussain, P. khan and Kwak kyung Sup, "WSN research activities for military application," 2009 11th International Conference on Advanced Communication Technology, pp. 271-274, 2009.

[4] A. Alaiad and L. Zhou, “Patients’ adoption of wsn-based smart home healthcare systems: an integrated model of facilitators and barriers,” IEEE Transactions on Professional Communication, vol. 60, no.1, pp. 4–23, 2017.

[5] V. T. Vu, T. V. Quyen, L. H. Truong, A. M. Le, C. V. Nguyen, and M. T. Nguyen, “Energy efficient approaches in wireless sensor networks,” ICSES Transactions on Computer Networks and Communications, vol. 6, no. 1, pp. 1–10, 2020.

[6] J. Wang, Y. Gao, W. Liu, A. K. Sangaiah, and H.-J. Kim, “Energy efficient routing algorithm with mobile sink support for wireless sensor networks,” Sensors, vol. 19, no. 7, p. 1494, 2019.

[7] X. Li, B. Keegan, F. Mtenzi, T. Weise and M. Tan, "Energy-Efficient Load Balancing Ant Based Routing Algorithm for Wireless Sensor Networks," in IEEE Access, vol. 7, pp. 113182-113196, 2019.

[8] M. Nguyen, H. Nguyen, A. Masaracchia, and C. Nguyen, “Stochastic-based power consumption analysis for data transmission in wireless sensor networks,” EAI Endorsed Transactions on Industrial Networks and Intelligent Systems, vol. 6, no. 19, 2019.

[9] NGUYEN, Minh Tuan and RAHNAVARD, Nazanin, "Cluster-Based Energy-Efficient Data Collection in Wireless Sensor Networks Utilizing Compressive Sensing," 2013 IEEE Military Communications Conference, pp. 1708-1713, 2013.

[10] Nguyen, M.T. and K. A. Teague, “Compressive sensing based random walk routing in wireless sensor networks,” Ad Hoc Networks, vol. 54, pp. 99–110, 2017.

[11] R. Huang, L. Ma, G. Zhai, J. He, X. Chu and H. Yan, "Resilient Routing Mechanism for Wireless Sensor Networks With Deep Learning Link Reliability Prediction," in IEEE Access, vol. 8, pp. 64857-64872, 2020.

[12] Nguyen, Minh Tuan, K. A. Teague, and N. Rahnavard, “CCS: Energy-efficient data collection in clustered wireless sensor networks utilizing block-wise compressive sensing,” Computer Networks, vol. 106, pp. 171–185, 2016.

[13] Nguyen, Minh T., L. H. Truong, T. T. Tran, and C.-F. Chien, “Artificial intelligence based data processing algorithm for video surveillance to empower industry 3.5,” Computers & Industrial Engineering, vol. 148, p. 106671, 2020.

[14] M. T. Nguyen and K. A. Teague, "Compressive sensing based energy-efficient random routing in wireless sensor networks," 2014 International Conference on Advanced Technologies for Communications (ATC 2014), pp. 187-192, 2014.

[15] Nguyen, M.T. and K. A. Teague, "Random sampling in collaborative and distributed mobile sensor networks utilizing compressive sensing for scalar field mapping," 2015 10th System of Systems Engineering Conference (SoSE), pp. 1-6, 2015.

[16] M. T. Nguyen, K. A. Teague and S. Bui, "Compressive wireless mobile sensing for data collection in sensor networks," 2016 International Conference on Advanced Technologies for Communications (ATC), pp. 437-441, 2016.

[17] C. Y. Tazibt, M. Bekhti, T. Djamah, N. Achir and K. Boussetta, "Wireless sensor network clustering for UAV-based data gathering," 2017 Wireless Days, pp. 245-247, 2017.

[18] H. T. Do, H. T. Hua, M. T. Nguyen, C. V. Nguyen, H. T. Nguyen, H. T. Nguyen, and N. T. Nguyen, “Formation control algorithms for multiple-uavs: a comprehensive survey,” EAI Endorsed Transactions on Industrial Networks and Intelligent Systems, vol. 8, no. 27, p. e3, 2021.

[19] M. T. Nguyen, “Energy harvesting in wireless sensor networks: benefits and challenges,” ICSES Interdisciplinary Transactions on Cloud Computing, IoT, and Big Data, vol. 4, no. 1, pp. 1–3, 2020.

[20] P.-F. Wu, F. Xiao, C. Sha, H.-P. Huang, R.-C. Wang, and N.-X. Xiong, “Node scheduling strategies for achieving full-view area coverage in camera sensor networks,” Sensors, vol. 17, no. 6, p. 1303, 2017.

[21] F. Viola, P. Romano, R. Miceli, G. Acciari and C. Spataro, "Piezoelectric model of rainfall energy harvester," 2014 Ninth International Conference on Ecological Vehicles and Renewable Energies (EVER), pp. 1-7, 2014.

[22] H. Sato and T. Yachi, "Harvesting electric power with a cane for radio communications," 2015 International Conference on Renewable Energy Research and Applications (ICRERA), pp. 292-295, 2015.

[23] J. Milanezi, J. P. C. L. da Costa and E. P. de Freitas, "Improved radiofrequency energy harvesting based on a rectenna array system and its feasibility evaluation in urban environments," 2014 International Conference on Renewable Energy Research and Application (ICRERA), pp. 561-565, 2014.

[24] G. de Carvalho Bertoli, G. M. Pacheco and G. J. Adabo, "Extending flight endurance of electric unmanned aerial vehicles through photovoltaic system integration," 2015 International Conference on Renewable Energy Research and Applications (ICRERA), pp. 143-147, 2015.

[25] R. Moghe, Y. Yang, F. Lambert and D. Divan, "A scoping study of electric and magnetic field energy harvesting for wireless sensor networks in power system applications," 2009 IEEE Energy Conversion Congress and Exposition, pp. 3550-3557, 2009.

[26] M. T. Nguyen and K. A. Teague, “Compressive sensing based random walk routing in wireless sensor networks,” Ad Hoc Networks, vol. 54, pp. 99–110, 2017.

[27] SAMN, Anas A. "Performance Evaluation and Parameter Sensitivityof Speed Bump Energy Harvester Passed by Various Vehicles", International Journal of Smart Grid-ijSmartGrid, pp.111-122, 2018.

[28] K. Gonchigsumlaa, Y.-i. Kim, and P. Bayarsaikhan, “Design and experiment of energy harvesting power supply for wireless sensor network in freight train monitoring,” International Journal of Precision Engineering and Manufacturing, vol. 21, no. 6, pp. 1135–1142, 2020.

[29] S. B. Jadhav and S. M. Lambor, "Hybrid solar and radio frequency (RF) energy harvesting," 2017 IEEE International Conference on Power, Control, Signals and Instrumentation Engineering (ICPCSI), pp. 1975-1980, 2017.

[30] C. Knight, J. Davidson, and S. Behrens, “Energy options for wireless sensor nodes,” Sensors, vol. 8, no. 12, pp. 8037–8066, 2008.

[31] Badal, F.R.; Subrata, K.S.; Sajal, K.D. Transient Stabilization Improvement of Induction Generator Based Power System using Robust Integral Linear Quadratic Gaussian Approach. Int. J. Smart Grid-ijSmartGrid , pp.73–83, 2019.

[32] C. V. Nguyen, M. T. Nguyen, T. V. Quyen, A. M. Le, A. Masaracchia, H. T. Nguyen, H. P. Nguyen, L. D. Nguyen, H. T. Nguyen, and V. Q. Nguyen, “Hybrid solar-rf energy harvesting systems for electric operated wheelchairs,” Electronics, vol. 9, no. 5, p. 752, 2020.

[33] P. T. V. Bhuvaneswari, R. Balakumar, V. Vaidehi and P. Balamuralidhar, "Solar Energy Harvesting for Wireless Sensor Networks," 2009 First International Conference on Computational Intelligence, Communication Systems and Networks, pp. 57-61, 2009.

[34] M. Hamza, M. U. Rehman, A. Riaz, Z. Maqsood and W. T. Khan, "Hybrid Dual Band Radio Frequency and Solar Energy Harvesting System for Making Battery-less Sensing Nodes," 2021 IEEE Radio and Wireless Symposium (RWS), pp. 116-118, 2021.

[35] J. Bito, R. Bahr, J. G. Hester, S. A. Nauroze, A. Georgiadis and M. M. Tentzeris, "A Novel Solar and Electromagnetic Energy Harvesting System With a 3-D Printed Package for Energy Efficient Internet-of-Things Wireless Sensors," in IEEE Transactions on Microwave Theory and Techniques, vol. 65, no. 5, pp. 1831-1842, May 2017.

[36] Khan, D., Oh, S. J., Yeo, S., Ryu, Y., In, S. H., Rad, R. E.,& Lee, K. Y, "A High-Efficient Wireless Power Receiver for Hybrid Energy-Harvesting Sources," in IEEE Transactions on Power Electronics, vol. 36, no. 10, pp. 11148-11162, Oct. 2021.

[37] H. Sharma, A. Haque and Z. A. Jaffery, "An Efficient Solar Energy Harvesting System for Wireless Sensor Nodes," 2018 2nd IEEE International Conference on Power Electronics, Intelligent Control and Energy Systems (ICPEICES), pp. 461-464, 2018.

[38] P. Sasikumar and S. Khara, "K-Means Clustering in Wireless Sensor Networks," 2012 Fourth International Conference on Computational Intelligence and Communication Networks, pp. 140-144, 2012.

[39] M. T. Nguyen, H. M. La and K. A. Teague, "Collaborative and Compressed Mobile Sensing for Data Collection in Distributed Robotic Networks," in IEEE Transactions on Control of Network Systems, vol. 5, no. 4, pp. 1729-1740, Dec. 2018.

[40] E. Khansalee, K. Nuanyai, and Y. Zhao, “A dual-band rectifier for rf energy harvesting,” Engineering Journal, vol. 19, no. 5, pp. 189–197,2015.

[41] G. Singh, F. Mumtaz, V. A. Bohara and A. Srivastava, "Experimental Observations on Hybrid RF-Solar Energy Harvesting Circuit for Low Power Applications," 2018 IEEE International Conference on Advanced Networks and Telecommunications Systems (ANTS), pp. 1-3, 2018.

[42] S. Roy, J. -J. Tiang, M. B. Roslee, M. T. Ahmed and M. A. P. Mahmud, "A Quad-Band Stacked Hybrid Ambient RF-Solar Energy Harvester With Higher RF-to-DC Rectification Efficiency," in IEEE Access, vol. 9, pp. 39303-39321, 2021.

[43] J. C. S. Kadupitiya, T. N. Abeythunga, P. D. M. T. Ranathunga and D. S. De Silva, "Optimizing RF energy harvester design for low power applications by integrating multi stage voltage doubler on patch antenna," 2015 8th International Conference on Ubi-Media Computing (UMEDIA), pp. 335-338, 2015.

[44] S. Shen, Y. Zhang, C. Chiu and R. Murch, "An Ambient RF Energy Harvesting System Where the Number of Antenna Ports is Dependent on Frequency," in IEEE Transactions on Microwave Theory and Techniques, vol. 67, no. 9, pp. 3821-3832, Sept. 2019.